Research Article
A Robust Control for an Aerial Robot Quadrotor under Wind Gusts

Li Ding [1,2] and Zhenwei Wang[1]

[1]*College of Mechanical Engineering, Jiangsu University of Technology, Changzhou 213001, China*
[2]*Department of Industrial and System Engineering, The Hong Kong Polytechnic University, 999077 Hung Hom, Hong Kong*

Correspondence should be addressed to Li Ding; nuaadli@163.com

A robust flight controller based on linear active disturbance rejection control (LADRC) is proposed for stability control of an aerial robot quadrotor under wind gusts. The nonlinear dynamical model of the quadrotor, considering the wind disturbance, is firstly established through Newton-Euler method. Subsequently, a robust LADRC technique is proposed to design the controllers for the inner loop and outer loop of the aircraft. In this control scheme, the linear extended state observer (LESO) serves as a compensator which can effectively reject the wind gusts. Then, a method of parameter tuning is introduced to obtain the optimized control performance. Finally, the effectiveness and advantages of the proposed controller are demonstrated through series of simulation case.

1. Introduction

Quadrotor is the most popular configuration of multirotor unmanned aerial robot, extensively for civilian applications [1, 2]. In recent years, significant growth of interest is witnessed towards the academic research of the quadrotor. This is possibly attributed to their certain features, such as simple mechanical structure, hovering, and agile maneuverability. With the increasing requirement of autonomous flight under different conditions, control of the quadrotor is an important challenge. Complex rotation and translation operations are also commonly encountered in the mathematical model, resulting in complex equations that have to be taken into account when designing control laws. On the other hand, the position control and attitude control of the quadrotor are extremely sensitive to external disturbance, such as wind gusts. Particularly, robustness issues may be critical for the control of quadrotor since they are subjected to the complicated dynamics and external disturbances. Several proper control methodologies for the quadrotor have been reported in the literatures, such as proportion integration differentiation (PID) control [3], backstepping control [4], sliding mode control [5], and model predictive control [6].

Nevertheless, there are a few researches about the robust control of the quadrotor, especially under the wind gusts.

In order to weaken the effect of wind gusts, some authors have proposed complicated control techniques to achieve stability. In the literatures [7, 8], adaptive controllers of different structures were verified by simulations and experiments on test bench. For control of a multirotor aircraft, Salazar et al. [9] proposed a novel mathematical model of the wind gusts and designed a simple nonlinear control law to resist the wind disturbance. The effect of wind disturbance was discussed towards the issue of (unmanned air vehicle) UAV path planning in the literatures [10, 11]. From the analysis, compensation control for the aircraft may be an effective method. Dong et al. [12] designed a flight controller with disturbance observer (DOB) to guarantee the high-performance trajectory tracking of a quadrotor. The DOB-based controller is robust to wind gusts without the use of high control gain or extensive computational power.

Our team has proposed in previous articles, like [13], the use of LADRC to control a small-scale unmanned helicopter. This control strategy is rooted in active disturbance rejection control (ADRC) which was firstly proposed by Han [14]. LADRC is a simplified implementation of the ADRC, in

which bandwidth is the only adjustable parameter of the control performance. A previous contribution from our team presented the parameter tuning towards the LADRC based on the artificial bee colony algorithm [15]. Detailed background and principles on the ABC can be found in the literatures [16, 17], and the authors analyzed the performance of the ABC on optimization problem.

The content is organized in the following manner: Section 2 presents the mathematical model of the quadrotor under the wind gusts. In Section 3, the robust controller is described using the LADRC strategy. And the proof of the stability analysis for the proposed controller is given in Section 4. A method of parameter tuning is applied in Section 5, to optimize the performance of our proposed controller. The control law with wind gusts is simulated and illustrated in Section 6. Finally, our conclusions and contributions are discussed in Section 7.

2. Mathematical Model

The free body diagram and coordinate systems for the quadrotor are given in Figure 1. It is controlled by the angular speeds of four electric motors. Each motor produces a thrust and a torque m_i $(i = 1, 2, 3, 4)$, whose combination generates the main thrust input U_1, pitch input U_2, roll input U_3, and yaw input U_4. Two reference frames are subjected to the quadrotor, namely, the earth-fixed frame $\{O_E X_E Y_E Z_E\}$ and the body-fixed frame $\{O_B X_B Y_B Z_B\}$. The position (x, y, z), attitude (pitch θ, roll ϕ and yaw ψ), and motion can be achieved through the two frames. According to Newton-Euler method. The six-degrees-of-freedom dynamics of the quadrotor are modeled as [18]

$$\ddot{x} = \frac{U_1 \left(c\psi s\theta c\phi + s\psi s\phi\right)}{m}$$

$$\ddot{y} = \frac{U_1 \left(s\psi s\theta c\phi - c\psi s\phi\right)}{m}$$

$$\ddot{z} = \frac{U_1 c\phi c\theta}{m} - g$$

$$\ddot{\phi} = \frac{U_2}{I_{xx}} + \frac{\dot{\theta}\dot{\psi}\left(I_{yy} - I_{zz}\right)}{I_{xx}} \quad (1)$$

$$\ddot{\theta} = \frac{U_3}{I_{yy}} + \frac{\dot{\phi}\dot{\psi}\left(I_{zz} - I_{xx}\right)}{I_{yy}}$$

$$\ddot{\psi} = \frac{U_4}{I_{zz}} + \frac{\dot{\phi}\dot{\theta}\left(I_{xx} - I_{yy}\right)}{I_{zz}}$$

where I_{xx}, I_{yy}, and I_{zz} are the moment of inertia, m is the mass, and g is the gravitational acceleration. And $s\alpha$ and $c\alpha$ are the abbreviations for $\cos\alpha$ and $\sin\alpha$.

The thrust of each propeller is calculated by $f_{m_i} = k_t \omega_i^2$ $(i = 1, 2, 3, 4)$ with k_t being the thrust coefficient and ω_i

Figure 1: Free body diagram of quadrotor.

Figure 2: Analysis of the main and lateral thrusts.

being the angular speeds. The relationship between the four inputs and angular speed is expressed by

$$\begin{bmatrix} U_1 \\ U_2 \\ U_3 \\ U_4 \end{bmatrix} = \begin{bmatrix} k_t & k_t & k_t & k_t \\ 0 & -k_t l & 0 & k_t l \\ -k_t l & 0 & k_t l & 0 \\ -k_m & k_m & -k_m & k_m \end{bmatrix} \begin{bmatrix} \omega_1^2 \\ \omega_2^2 \\ \omega_3^2 \\ \omega_4^2 \end{bmatrix} \quad (2)$$

where l denotes the distance from the center of mass to the center of the propeller and k_m is termed as antitorque coefficient.

In the outdoor flight, the quadrotor is generally exposed to lateral wind gusts. The aircraft will be yawed or overturned if it is subjected to the lateral wind gusts. Stating precisely, this leads to additional lateral air flow acting on the propeller, as shown in Figure 2. Hence, the total thrust $f_{T_i} = f_{m_i} + f_{w_i}$ $(i = 1, 2, 3, 4)$ could be described as [19]

$$f_{T_i} = 2\rho A \widehat{V} V_p \quad (3)$$

where ρ is the air density and A is the propeller area. V_p is the induced wind speed of the propeller and $\widehat{V}$ is the total wind induced speed of the rotor. The relationship between them is given by

$$\widehat{V} = \left[\left(V_w \cos\alpha + V_p \right)^2 + \left(V_w \sin\alpha \right)^2 \right]^{1/2} \tag{4}$$

where α represents the angle between the propeller axis and the lateral wind gusts. Since the latter is perpendicular to the former, $\alpha = 90°$. At this moment, the additional lateral forces are expressed by

$$f_{w_i} = 2\rho A V_p^2 \left(1 + \frac{V_w^2}{V_p^2} \right)^{1/2} - f_{m_i} \tag{5}$$

Moreover, the aerodynamics drag is defined as $m_{drag} = \rho A V_w^2 / 2 = k_{drag} V_w^2$, where $k_{drag} > 0$ is a constant depending on the parameter ρ, shape of the blade, and other factors. When the aircraft is disturbed by the lateral wind gusts, the additional torques acting on the propellers are represented by

$$\begin{bmatrix} m_{w_\phi} \\ m_{w_\theta} \\ m_{w_\psi} \end{bmatrix} = \begin{bmatrix} \left(f_{w_4} - f_{w_2} \right) l \\ \left(f_{w_3} - f_{w_1} \right) l \\ \sum_{i=1}^{4} m_{drag_i} \end{bmatrix} \tag{6}$$

Using (1), (5), and (6), the integrated quadrotor dynamical model can be rewritten as

$$\ddot{x} = \frac{U_1 \left(c\psi s\theta c\phi + s\psi s\phi \right)}{m} + \sum_{i=1}^{4} \frac{f_{w_i}}{m}$$

$$\ddot{y} = \frac{U_1 \left(s\psi s\theta c\phi - c\psi s\phi \right)}{m} + \sum_{i=1}^{4} \frac{f_{w_i}}{m}$$

$$\ddot{z} = \frac{U_1 c\phi c\theta}{m} - g + \sum_{i=1}^{4} \frac{f_{w_i}}{m}$$

$$\ddot{\phi} = \frac{U_2}{I_{xx}} + \frac{\dot{\theta}\dot{\psi} \left(I_{yy} - I_{zz} \right)}{I_{xx}} + \frac{m_{w_\phi}}{I_{xx}} \tag{7}$$

$$\ddot{\theta} = \frac{U_3}{I_{yy}} + \frac{\dot{\phi}\dot{\psi} \left(I_{zz} - I_{xx} \right)}{I_{yy}} + \frac{m_{w_\theta}}{I_{yy}}$$

$$\ddot{\psi} = \frac{U_4}{I_{zz}} + \frac{\dot{\phi}\dot{\theta} \left(I_{xx} - I_{yy} \right)}{I_{zz}} + \frac{m_{w_\psi}}{I_{zz}}$$

3. Robust Controller Design

According to (7), the input and output of each control channel present second-order derivative relation. Thus, we use the second-order system in the following form for describing the LADRC:

$$\ddot{x}_s = f_s \left(x_s, \dot{x}_s, w_s, t \right) + b(t) u$$
$$y_s = x_s \tag{8}$$

where u and y_s denote input and output, respectively. f_s is the external disturbance. x_s is state variables and $b(t)$ is the control function.

Suppose b_0 is the approximate value of $b(t)$, and (8) is written equivalently as

$$\ddot{x}_s = f_s \left(x_s, \dot{x}_s, w_s, t \right) + b_0 u = f_s + b_0 u$$
$$y_s = x_s \tag{9}$$

By rewriting the above equation in the form of differential equation, one has

$$\dot{x}_{s_1} = x_{s_2}$$
$$\dot{x}_{s_2} = x_{s_3} + b_0 u$$
$$\dot{x}_{s_3} = h \tag{10}$$
$$y_s = x_{s_1}$$

with $x_{s_3} = f_s$ added as an augmented state and $h = \dot{f}_s$ as unknown disturbance. Now f_s can be estimated through a state observer based on a state space model:

$$\dot{\mathbf{x}} = \mathbf{A}\mathbf{x} + \mathbf{B}u + \mathbf{E}h$$
$$\mathbf{y} = \mathbf{C}\mathbf{x} \tag{11}$$

where

$$\mathbf{A} = \begin{bmatrix} 0 & 1 & 0 \\ 0 & 0 & 1 \\ 0 & 0 & 0 \end{bmatrix},$$

$$B = \begin{bmatrix} 0 \\ b_0 \\ 0 \end{bmatrix},$$

$$\mathbf{C} = \begin{bmatrix} 1 \\ 0 \\ 0 \end{bmatrix}, \tag{12}$$

$$\mathbf{E} = \begin{bmatrix} 0 \\ 0 \\ 1 \end{bmatrix}$$

The LESO of (11) can be constructed as

$$\dot{\mathbf{z}} = \mathbf{A}\mathbf{z} + \mathbf{B}u + \mathbf{L} \left(\mathbf{y} - \widehat{\mathbf{y}} \right)$$
$$\widehat{\mathbf{y}} = \mathbf{C}\mathbf{z} \tag{13}$$

where $\mathbf{L}$ is the observer gain. It is calculated as [17]

$$\mathbf{L} = \begin{bmatrix} l_1 \\ l_2 \\ l_3 \end{bmatrix} = \begin{bmatrix} \alpha_1 \omega_o \\ \alpha_2 \omega_o^2 \\ \alpha_3 \omega_o^3 \end{bmatrix} \tag{14}$$

where $\omega_o > 0$ is the observer bandwidth. It results in the characteristic polynomial of (13) being

$$\lambda(s) = s^3 + \alpha_1 s^2 + \alpha_2 s + \alpha_3 = (s + \omega_o)^3 \quad (15)$$

From the polynomial, one obtains

$$\alpha_1 = 3,$$
$$\alpha_2 = 3, \quad (16)$$
$$\alpha_3 = 1$$

The observer can track the state variables with well-tuned observer bandwidth and yield $z_1(t) \longrightarrow \hat{y}(t)$, $z_2(t) \longrightarrow \dot{\hat{y}}(t)$, and $z_3(t) \longrightarrow f_s$.

With the estimate of f_s, the LADRC can actively compensate for effect of the external disturbance in real time as

$$u = \frac{u_0 - z_3}{b_0} \quad (17)$$

The closed-loop control system is converted into a unit double integral plant. And the control law is [20, 21]

$$\ddot{y} = f - z_3 + u_0 \approx u_0 = \lambda_1 (r_e - z_1) - \lambda_2 z_2 \quad (18)$$

where r_e is the reference signal.

The transfer function of the second-order plant is given as

$$G_2 = \frac{\lambda_1}{s^2 + \lambda_2 s + \lambda_1} \quad (19)$$

Here, the gains can be calculated as [17]

$$\lambda_1 = \omega_c^2,$$
$$\lambda_2 = 2\omega_c \quad (20)$$

4. Stability Analysis

Define the error as

$$\mathbf{e} = \mathbf{x} - \mathbf{z} \quad (21)$$

Subtracting (13) from (11), the error equation is obtained as

$$\dot{\mathbf{e}} = \mathbf{A}_e \mathbf{e} + \mathbf{Eh} \quad (22)$$

where

$$\mathbf{A}_e = \mathbf{A} - \mathbf{LC} = \begin{bmatrix} -l_1 & 1 & 0 \\ -l_2 & 0 & 1 \\ -l_3 & 0 & 0 \end{bmatrix} \quad (23)$$

Obviously, the LESO is bounded-input bounded-output (BIBO) stable if the roots of the characteristic polynomial, namely (15), are all in the left half plane and $\mathbf{h}$ is bounded.

Theorem 1. *The design of LADRC from (13) to (18) yields a BIBO stable closed-loop system if the LESO and the control law for the unit double integral plant are stable.*
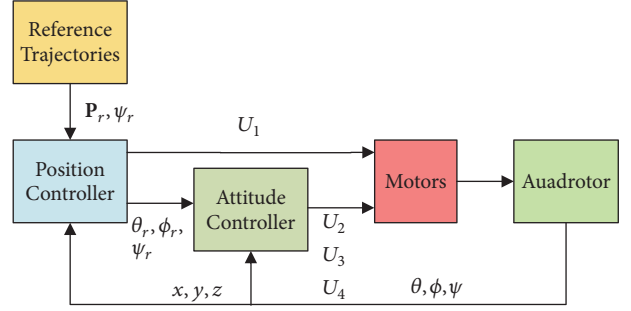
FIGURE 3: Control system architecture of the quadrotor.

Proof. According to (17) and (18), one has

$$u = \frac{1}{b_0} \begin{bmatrix} -\lambda_1 & -\lambda_2 & -1 \end{bmatrix} \begin{bmatrix} z_1 - r_e \\ z_2 \\ z_3 \end{bmatrix} = \mathbf{Qz} - \frac{1}{b_0} \begin{bmatrix} r_e \\ 0 \\ 0 \end{bmatrix} \quad (24)$$

$$= \mathbf{Qz} - \mathbf{G}$$

where

$$\mathbf{Q} = \frac{1}{b_0} \begin{bmatrix} -\lambda_1 & -\lambda_2 & -1 \end{bmatrix} \quad (25)$$

The closed-loop control system is rewritten as

$$\dot{\mathbf{x}} = \mathbf{Ax} + \mathbf{Bu} + \mathbf{Eh} = \mathbf{Ax} + \mathbf{BQz} - \mathbf{BG} + \mathbf{Eh} \quad (26)$$

$$\dot{\mathbf{z}} = \mathbf{Az} + \mathbf{Bu} + \mathbf{L}(\mathbf{y} - \hat{\mathbf{y}})$$
$$= \mathbf{LCx} + (\mathbf{A} - \mathbf{LC} + \mathbf{BQ})\mathbf{z} - \mathbf{BG} \quad (27)$$

Using the state space equation to represent the closed-loop control system, one gets

$$\begin{bmatrix} \dot{\mathbf{x}} \\ \dot{\mathbf{z}} \end{bmatrix} = \begin{bmatrix} \mathbf{A} & \mathbf{BQ} \\ \mathbf{LC} & \mathbf{A} - \mathbf{LC} + \mathbf{BQ} \end{bmatrix} \begin{bmatrix} \mathbf{x} \\ \mathbf{z} \end{bmatrix} + \begin{bmatrix} -\mathbf{B} & \mathbf{E} \\ -\mathbf{B} & \mathbf{0} \end{bmatrix} \begin{bmatrix} \mathbf{G} \\ \mathbf{h} \end{bmatrix} \quad (28)$$

Similarly, the control system is BIBO stable if the eigenvalues of (28) are in the left half plane. Since the reference signal r_e is always bounded, with the condition that the disturbance f_s satisfies differentiable, $\mathbf{h}$ is bounded. □

5. Parameter Tuning

According to the previous analysis, the control structure of the quadrotor is divided into two loops, i.e., inner loop and outer loop. The block diagram of such a structure is schematically shown in Figure 3. In the outer loop, the position vector $\mathbf{P}_r$ and yaw angle ψ_r are chosen as the reference signals. In the inner loop, the reference signal $(\theta_r, \phi_r, \psi_r)$ comes from the outer loop. Moreover, the four inputs generated by the two loops are converted into the angular speeds of motors.

The evaluation function is crucial for the parameter tuning. Consequently, an improved integral of time multiplied by absolute error (IITAE) is employed as performance index.
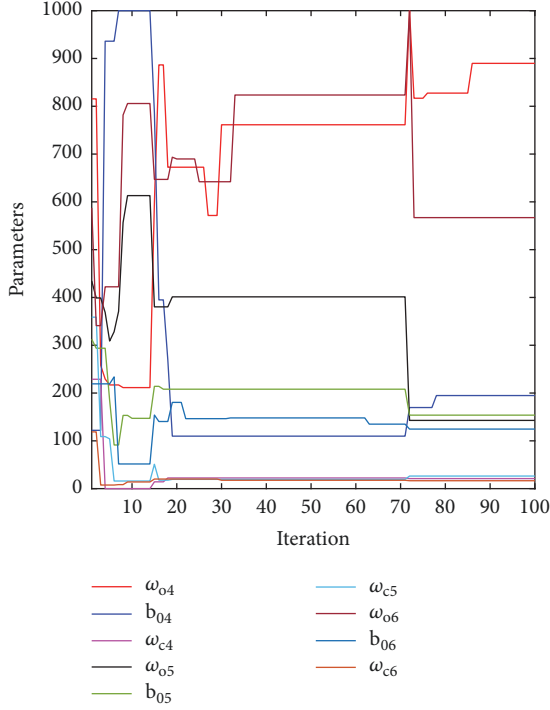
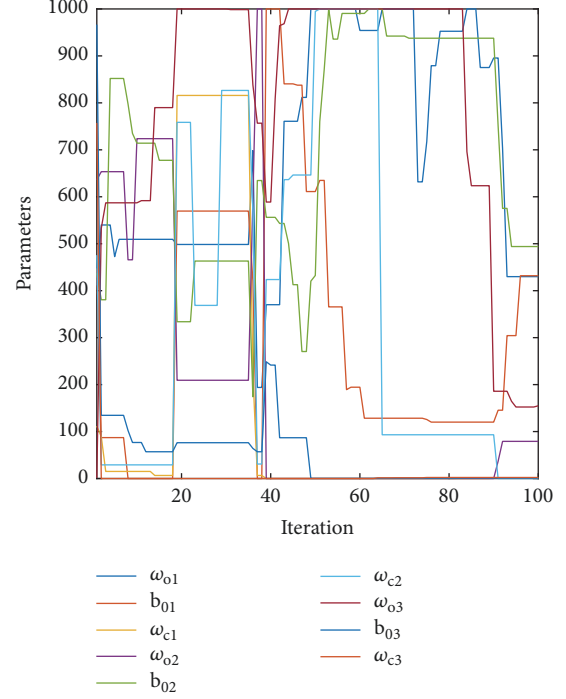FIGURE 4: Evolving curves of the control parameters.
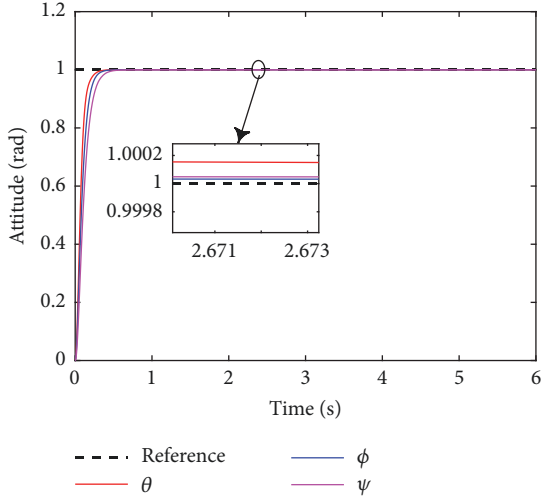

FIGURE 6: Tuned parameters of outer loop controller.

FIGURE 5: Response of the attitude.

The evaluation function of the performance index is defined as

$$F(t) = \alpha_1 \int_0^\infty t\, |e(t)|\, dt + \alpha_2 \int_0^\infty (u(t))^2\, dt + \alpha_3 t_s \\ + \alpha_4 o \tag{29}$$

where $e(t)$ is the error signal in the time domain, t_s is the settling time, o_s is the overshoot, and α_1, α_2, α_3, and α_4 are the weight coefficients. Note that the parameter tuning of the LADRC is conducted by the ABC algorithm, and the

TABLE 1: Physical parameters.

Item	Quantity
L (m)	0.2053
m (kg)	1.923
I_{xx} (kg·m^2)	0.094
I_{yy} (kg·m^2)	0.094
I_{zz} (kg·m^2)	0.086

exhaustive process is reported in the literature [13], and here repeating is unnecessary.

As taking the inner loop as an instance, the reference signal is set to 1 rad, 1 rad, 1 rad. There are three second-order LADRC in the inner loop, i.e., θ-LADRC, ϕ-LADRC, and ψ-LADRC. The physical parameters of the quadrotor are listed in Table 1. We use the ABC algorithm to tune the unknown control parameters under a unit step response case. The number of the iterations is 100. In addition, the simulation parameters of the wind gusts are given as $\rho = 1.293$ g/L, $A = 0.0016$ m^2, $V_P = 2$ m/s, and $V_w = 6$ m/s. And a white noise with the amplitude of 0.2 rad is added to the measured ports. The simulation time lasts for 6 s. Figure 4 displays the evolving curves of the control parameters, which indicates the process of the parameter tuning by ABC. The attitude response is shown in Figure 5. It is obvious that the LADRC has a satisfactory performance of wind resistance, and the steady state error is less than 2%. Furthermore, the responses of the three attitude channels are fast and accurate.
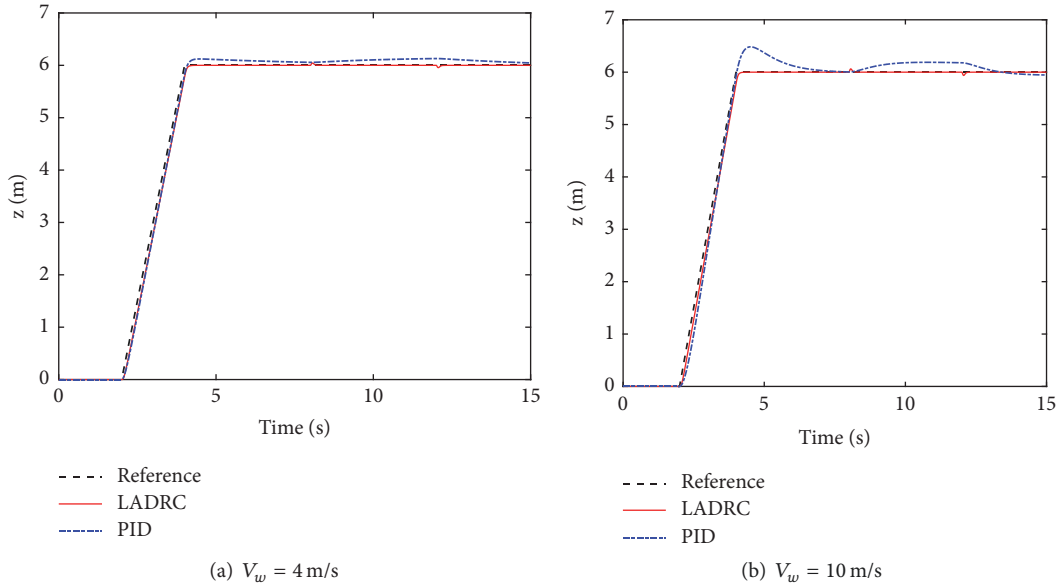
(a) $V_w = 4\,\text{m/s}$

(b) $V_w = 10\,\text{m/s}$

FIGURE 7: Position response under different wind gusts.
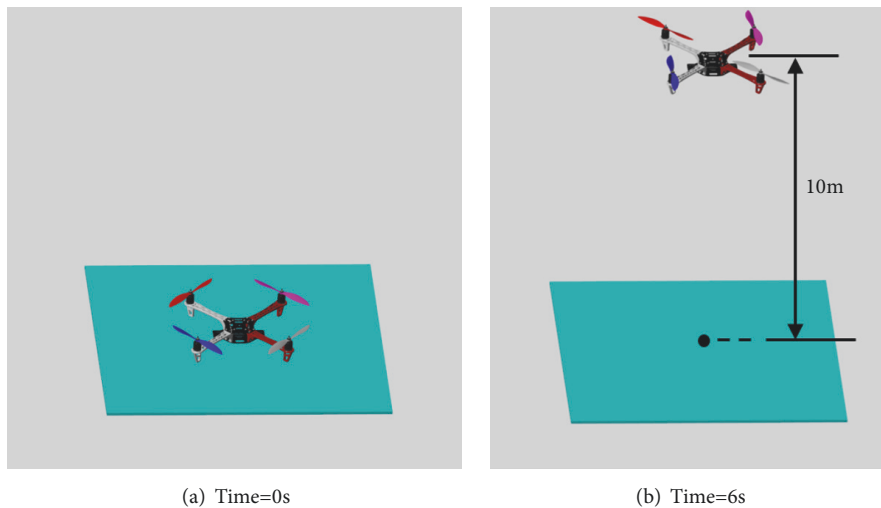

(a) Time=0s

(b) Time=6s

FIGURE 8: Hovering control in Simscape environment.

6. Simulation Results

In order to validate the robustness and wind resistance of the proposed control scheme for stabilizing the quadrotor at trajectory tracking, the simulation is conducted in MATLAB 2017a programming environment on an Intel Core i7-4720 PC running Windows 10. Similarly, random wind gusts are added to the input of the outer loop.

As pointed out in Section 5, the control parameters of the outer loop controller are also tuned by the ABC algorithm. The tuned parameters are shown in Figure 6 using a unit step response case.

Moreover, we introduce a PID controller from the literature [22] as a comparison to test the robustness of our proposed controller. In the comparative simulation, the quadrotor follows a referenced trajectory of z direction as

shown in Figure 7. Meanwhile, lateral wind gusts are applied with different wind speeds at a specific time period 8 s-12 s. The PID and LADRC are applied to stabilize the position of the aircraft, respectively. From the result, the response of LADRC is slightly faster than that of PID. As the wind speed increases, the tracking error becomes bigger. Nevertheless, it is obvious that the steady state error of LADRC is smaller than that of PID due to the LESO. In conclusion, the LADRC has a strong ability of wind disturbance compensation.

Lastly, a visual simulation is run in the MATALB/ Simscape environment to display the trajectory tracking of the quadrotor. Note that the Simscape link utility creates a physical modeling XML file that represents the quadrotor's parts as bodies and maps the constraints between the parts into joints [23]. In this case, the task requires that the quadrotor takes off from the ground and flies in hover. The

simulation time lasts for 8s. From the result in Figure 8, the quadrotor has a stable flight performance based on the proposed controller.

7. Conclusion

A new LADRC control scheme is given for the stability control of an aerial robot quadrotor under wind gusts in this article. The proposed controller roughly has two parts: the LESO part applied to properly estimate and compensate the wind disturbance leading to an attractive model-free feature and a PD part applied to ensure satisfactory control performance. Moreover, corresponding stability of the closed-loop control plant is analyzed and an ABC algorithm is applied for parameter tuning of the LADRC. Finally, all the simulation results show the proposed controller has a better ability of resisting wind gusts comparing to the traditional PID.

In the future, more advanced control strategies such as that reported in the literature [24] will be studied to control the movement of the quadrotor under wind gusts.

Data Availability

Figure 4 displays the variation of the tuning parameters. There is no need to give the detailed parameters searched by ABC. In addition, the data of quadrotor is listed in Table 1.

Conflicts of Interest

The authors declare that they have no conflicts of interest.

Acknowledgments

References

[1] R. Amin, L. Aijun, and S. Shamshirband, "A review of quadrotor UAV: Control methodologies and performance evaluation," *International Journal of Automation and Control Engineering*, vol. 10, no. 2, pp. 87–103, 2016.

[2] M. A. Tofigh, M. J. Mahjoob, and M. Ayati, "Dynamic modeling and nonlinear tracking control of a novel modified quadrotor," *International Journal of Robust and Nonlinear Control*, vol. 28, no. 2, pp. 552–567, 2018.

[3] S. An, S. Yuan, and H. Li, "Self-tuning of PID controllers design by adaptive interaction for quadrotor UAV," in *Proceedings of the 7th IEEE Chinese Guidance, Navigation and Control Conference, CGNCC 2016*, pp. 1547–1552, IEEE, Xiamen, China, August 2016.

[4] A. Das, F. Lewis, and K. Subbarao, "Backstepping approach for controlling a quadrotor using lagrange form dynamics," *Journal of Intelligent & Robotic Systems*, vol. 56, no. 1-2, pp. 127–151, 2009.

[5] D. Lee, H. J. Kim, and S. Sastry, "Feedback linearization vs. adaptive sliding mode control for a quadrotor helicopter," *International Journal of Control, Automation, and Systems*, vol. 7, no. 3, pp. 419–428, 2009.

[6] A. Chamseddine, Y. Zhang, C.-A. Rabbath, C. Fulford, and J. Apkarian, "Model reference adaptive fault tolerant control of a quadrotor UAV," in *Infotech@ Aerospace*, St. Louis, MO, USA, March 2011.

[7] F. Chen, F. Lu, B. Jiang, and G. Tao, "Adaptive compensation control of the quadrotor helicopter using quantum information technology and disturbance observer," *Journal of The Franklin Institute*, vol. 351, no. 1, pp. 442–455, 2014.

[8] S. Salazar, H. Romero, R. Lozano et al., "Modeling and real-time stabilization of an aircraft having eight rotors," *Journal of Intelligent and Robotic Systems*, vol. 54, no. 1-3, pp. 455–470, 2008.

[9] L. Ding, R. Ma, H. Wu, C. Feng, and Q. Li, "Yaw control of an unmanned aerial vehicle helicopter using linear active disturbance rejection control," *Proceedings of the Institution of Mechanical Engineers, Part I: Journal of Systems and Control Engineering*, vol. 231, no. 6, pp. 427–435, 2017.

[10] S. Jackson, J. Tisdale, M. Kamgarpour, B. Basso, and J. K. Hedrick, "Tracking controllers for small UAVs with wind disturbances: theory and flight results," in *Proceedings of the 47th IEEE Conference on Decision and Control (CDC '08)*, pp. 564–569, IEEE, Cancun, Mexico, December 2008.

[11] A. L. Jennings, R. Ordóñez, and N. Ceccarelli, "An ant colony optimization using training data applied to UAV way point path planning in wind," in *Proceedings of the 2008 IEEE Swarm Intelligence Symposium, SIS 2008*, USA, September 2008.

[12] W. Dong, G.-Y. Gu, X. Zhu, and H. Ding, "High-performance trajectory tracking control of a quadrotor with disturbance observer," *Sensors and Actuators A: Physical*, vol. 211, pp. 67–77, 2014.

[13] J. Song, Z. Gan, and J. Han, "Study of active disturbance rejection controller on filtering," *Control and Decision*, vol. 18, no. 1, pp. 110–112, 2003.

[14] D. Ma, Y. Xia, T. Li, and K. Chang, "Active disturbance rejection and predictive control strategy for a quadrotor helicopter," *IET Control Theory & Applications*, vol. 10, no. 17, pp. 2213–2222, 2016.

[15] D. Karaboga, "An idea based on honey bee swarm for numerical optimization," Technical report-tr06, Erciyes university, engineering faculty, computer engineering department, Kayseri, Turkey, 2005.

[16] L. Ding, H. Wu, Y. Yao, and Y. Yang, "Dynamic model identification for 6-DOF industrial robots," *Journal of Robotics*, vol. 2015, Article ID 471478, pp. 1–9, 2015.

[17] N. Michael, D. Mellinger, Q. Lindsey, and V. Kumar, "The GRASP multiple micro-UAV testbed," *IEEE Robotics and Automation Magazine*, vol. 17, no. 3, pp. 56–65, 2010.

[18] Y. Guo, B. Jiang, and Y. Zhang, "A novel robust attitude control for quadrotor aircraft subject to actuator faults and wind gusts," *IEEE/CAA Journal of Automatica Sinica*, vol. 5, no. 1, pp. 292–300, 2018.

[19] Z. Gao, "Scaling and bandwidth-parameterization based controller tuning," in *Proceedings of the American Control Conference*, pp. 4989–4996, Denver, Colo, USA, June 2003.

[20] Z. Gao, "Active disturbance rejection control: a paradigm shift in feedback control system design," in *Proceedings of the American Control Conference*, pp. 2399–2405, Minneapolis, Minn, USA, June 2006.

[21] Y. Liu, J. Liu, and S. Zhou, "Linear active disturbance rejection control for pressurized water reactor power," *Annals of Nuclear Energy*, vol. 111, pp. 22–30, 2018.

[22] W. Dong, G. Gu Y, X. Zhu et al., "Modeling and control of a quadrotor UAV with aerodynamic concepts," in *Proceedings of World Academy of Science, Engineering and Technology*, vol. 77, p. 437, World Academy of Science, Engineering and Technology (WASET), 2013.

[23] https://ww2.mathworks.cn/help/physmod/simscape/index .html?s_tid=srchtitle.

[24] L. Fortuna and G. Muscato, "A roll stabilization system for a monohull ship: modeling, identification, and adaptive control," *IEEE Transactions on Control Systems Technology*, vol. 4, no. 1, pp. 18–28, 1996.

International Journal of
Rotating
Machinery

The Scientific
World Journal

Journal of
Sensors

Advances in
Multimedia

Journal of
Engineering

Advances in
Civil Engineering

Journal of
Control Science
and Engineering

Journal of
Robotics

Journal of
Electrical and Computer
Engineering

Hindawi

Submit your manuscripts at
www.hindawi.com

Advances in
OptoElectronics

VLSI Design

International Journal of
Navigation and
Observation

Modelling &
Simulation
in Engineering

International Journal of
Aerospace
Engineering

International Journal of
Chemical Engineering

International Journal of
Antennas and
Propagation

Active and Passive
Electronic Components

Shock and Vibration

Advances in
Acoustics and Vibration